Finite Element Analysis of Two-step Deep Rolling of Bearing Steel for Expansion and Equalization of Compressive Residual Stress Profiles

Joshua Simon[1], Jürgen Gegner[2,3]

[1] *Faculty of Applied Natural Sciences and Humanities, University of Applied Science Würzburg-Schweinfurt, joshsimon96@googlemail.com*

[2] *Department of Material Physics, SKF GmbH, juergen.gegner@skf.com*

[3] *Institute of Materials Science and Materials Testing, University of Siegen, juergen.gegner@uni-siegen.de*

Abstract – Deep rolling for prevention of frictional cracking and fatigue failure enjoys growing popularity in bearing applications. The conventional process suffers from an outer layer low in compressive residual stress. With decreasing tool diameter, the unwanted skin but also the desired influence depth diminish. Simply enhancing the force acting on a small body to move the impact zone farther into the workpiece is no effective remedy, above all because of excessively rising compressive residual stresses. In the present paper, two-step deep rolling with differently sized and loaded tools is introduced as corrective measure against the weak surface layer. For assessing the influence of process parameters, a finite element analysis is performed on ANSYS 19.2 software. A two-dimensional model of the rolling elements pressed onto a raceway is used for residual stress simulation and engineering. Material response of bearing steel is described by isotropic bilinear elastic-plastic behaviour in the von Mises yield criterion. Initial condition is free of (residual) stress. Reference simulations of single overrolling events reproduce experimental findings. Residual stress redistribution is more complex after the second pass. Four parameter studies are conducted to explore two-step deep rolling. The degree of expansion of the impact width of compressive residual stresses depends on the difference in tool diameter. Simulations furthermore indicate benefit from applying the large rolling element first. Effective shape equalization of the compressive residual stress depth profile is basically promoted by similar Hertzian pressure in both process stages.

Keywords – deep rolling, finite element analysis, residual stress engineering, process development, bearing steel

1. Introduction

Cold working mechanical surface treatments are widely applied to improve fatigue strength and damage tolerance of metal components by inducing compressive residual stresses. Radial Hertzian pressure loading essentially governs deformation by deep rolling, whereas shot peening additionally causes plastic stretching near the surface in response to tangential forces from multiple projectile impacts. Consequential differing development of compressive residual stresses becomes obvious from a comparison of typical depth distributions measured by X-ray diffraction in hardened high strength bearing steel. In Figure 1, the initial state after machining is plotted schematically for reference as well. Deep rolling compressive residual stresses can extend significantly further into the material but are rather low in the outer layer. Although the surface value of about 400 MPa benefits from previous honing, it is considerably lower than approx. 700 MPa after shot peening. Dominant Hertzian pressure effect is reflected in pronounced subsurface compressive residual stress maxima. The size of bombarding particles ($1^{\pm 0.2}$ mm in Figure 1) limits shot peening influence depth.

In recent years, deep rolling has attracted increasing attention for bearing application [1–4]. In contrast to shot peening, which requires subtractive reworking of impact crater waviness (typical R_a roughness of several µm), the burnishing process even boosts surface quality [5]. For assessing life gain in classical rolling contact fatigue on the basis of materials science, it should be considered that compressive residual stresses impede butterfly crack initiation and wing growth occurring under Hertzian pressure p_0 upwards of around 1300 MPa [6], but on the other hand arise independently after few ring revolutions in operation once cyclic (micro) plasticity sets in [1], i.e. at p_0 above 2500 to 3000 MPa. With similar deep rolling pre-treatment, bearing tests provide greater enhancement in the load range 1300 MPa$\leq p_0 \leq$2500 MPa than for $p_0 \geq$3200 MPa [2,3]. Larger effect for roller than ball contact is indicated by the corresponding size of damage risk volume [4]. Higher resistance against spontaneous surface cracking by compressive residual stresses is verified experimentally as well [7].

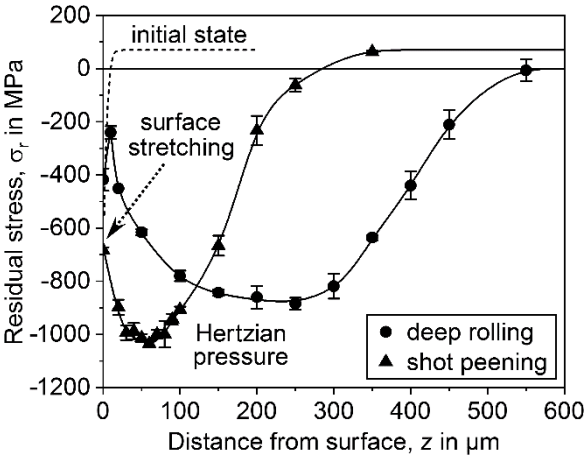

Figure 1: Depth distributions of circumferential residual stress (initial state indicated) after deep rolling and shot peening of surface machined bearing rings out of martensitically hardened 100Cr6 steel.

As the weaker boundary zone (see Figure 1) diminishes improvability of cyclic and static load capacity by deep rolling, corrective measures have been proposed in the literature. The most direct approach is to

remove the near-surface layer up to the peak value of compressive residual stress by subsequent machining [8]. Even if less material is taken off, however, the involved decrease of strengthening depth may be unacceptable particularly for larger bearings. Combined deep rolling and shot peening [9], as suggested by Figure 1, avoids this drawback. Due to resulting surface roughening, the method is inappropriate for bearing applications unless final machining is likewise performed. The alternative of a second deep rolling step at reduced Hertzian pressure with more overturns circumvents this problem [10]. Note that multiple impacts at the same spot increase the subsurface compressive residual stresses from shot peening (cf. Figure 1). It is reported that the maximum is reached rapidly after few collisions [11], which agrees well with findings on repeated deep rolling [1,12]. Because of closer proximity to surface, it is also important that rising number of passes significantly broadens the compressive residual stress distribution [1,13].

In the present paper, another multi-stage deep rolling process is examined. The aim of the study is to estimate numerically the potential for producing a more uniform edge profile of compressive residual stresses. By successively applying rolling elements of different diameter [14], the outer and deeper region can be influenced specifically. Modelling of deep rolling for simulation aided compressive residual stress engineering is based on the triaxially loaded Hertzian contact between two bodies. In the analytical theory, elastic solids and low strains are assumed. A finite element analysis is therefore carried out to involve plastic deformation and residual stress generation.

2. Finite element modelling of a two-step deep rolling process

A measurement based experimental approach to residual stress optimization is a difficult and time-consuming task. Before starting trials, therefore, a finite element analysis (FEA) is an appropriate preparation tool to better understand the effect of process parameters. For this purpose, a two-dimensional (2D) model of multi-step deep rolling is established. The considered plane geometry comprises the raceway to be treated and two rolling bodies. The FEA model is built using the commercial finite element software ANSYS 19.2 with its mechanical APDL solver, as also used for the computation and processing of all results presented in the following. The simulation aims to provide information on the compressive residual stresses during the passes over the hardened steel raceway and the influence of various parameters, such as size of the rolling elements, load and order of application. As discussed above, overrolling with sufficient contact pressure leaves an outer skin of lower compressive residual stress ahead of the subsurface peak. This is in response to the course of von Mises equivalent stress for radial Hertzian loading. If the rolling element size is chosen small to reduce the extent of the border, the desired in-depth effect diminishes accordingly. A large diameter, on the other hand, creates a pronounced weak edge zone. This fundamental restriction is addressed by the examined multi-step process.

Deep rolling can be viewed as a simplified contact problem. Numerical effort and calculation methods are affected by its highly nonlinear nature [15]. ANSYS offers a powerful range of contact tools to carry out such a stress analysis. Deep rolling finite element simulations are available in the recent literature [13,16–18], for instance referring to automotive crankshafts or railway axles.

2.1. Geometries and meshing

For the sake of saving computation time, a 2D model is used to numerically investigate two-pass deep rolling. The reason is that this preliminary study of process development serves the rather qualitative purpose of estimating how the application of differently sized and loaded rolling bodies can influenced the near-surface compressive residual stress state. More practical aspects, such as dealing with overlap or varying track widths of ball tools, are not yet of interest. The model consists of one linear raceway and two circular rolling elements. The latter represent the working tools. To capture the multi-step process in a single simulation, these two rolling elements are superimposed in the model with individual meshes. Note therefore that they represent separate bodies. The raceway reveals a much finer mesh than the rolling elements as the resulting stresses in the workpiece are of primary interest. Figure 2 shows the model geometry. For increased computational accuracy, the mesh of the raceway element (overall thickness: 3.3 mm) is further refined towards the centre of Hertzian contact.

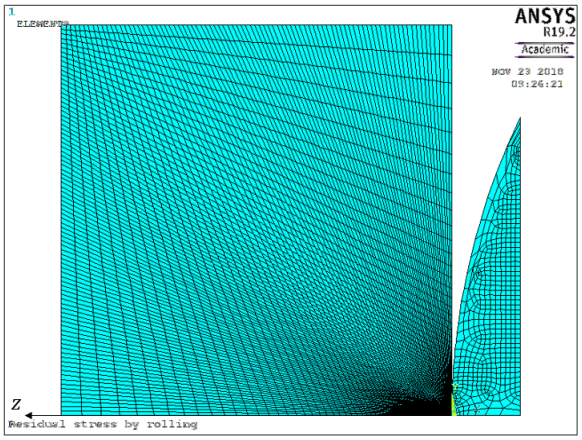

Figure 2: Meshed 2D Model with raceway segment on the left and two overlapping rolling elements (sectors) on the right. The z-axis is directed into the depth of the workpiece.

2.2. Material

All geometries in the model are assigned to bearing steel but with varying Young's modulus E. Higher stiffness (E=300 GPa is a typical value for a ceramic tool) reduces deformation of the rolling elements. The basic material data are given in Table 1. The mechanical behaviour of the bearing steel is characterised in the simulation by an isotropic bilinear elastic-plastic model. Figure 3 schematically illustrates the simplified stress σ vs. strain ε relationship. Note that yield and ultimate strength, $R_{p0.2}$ and R_m, respectively depend on

heat treatment and mechanical processing. Both values set in Table 1 fall in the upper range of bearing steel.

Table 1: Material properties of the raceway (workpiece) and, where mentioned, the rolling elements (tools).

Young's modulus	200 GPa
Young's modulus, rolling elements	300 GPa
Yield strength	2100 MPa
Ultimate strength	2600 MPa
Poisson's ratio	0.3

The residual stresses are calculated by means of the von Mises yield criterion, which is usually chosen in plasticity models. In particular, it describes material response to static and cyclic Hertzian compression appropriately [19,20]. Note that deep rolling residual stresses are caused by local non-uniform micro-plastic deformation.

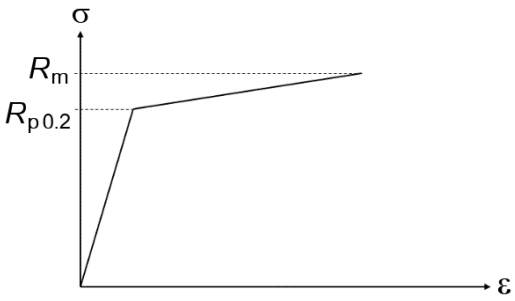

Figure 3: Bilinear elastic-plastic stress-strain curve, yield point and ultimate strength are indicated.

2.3. Contact formulation

Friction is not considered. The core of the simulation is the contact problem between the raceway and rolling element. Its solution is highly complex. The contact formulation comprises the mathematical description of the geometry and the numerical approach. ANSYS provides several algorithms for this purpose. For a Hertzian type contact problem, such as deep rolling, either the pure penalty or augmented Lagrange method are suitable [21]. The former is used as calculation algorithm for the simulation because it leads to good results in practice. This approach also saves computation time due to lower numerical complexity. Contact detection occurs by means of the surface projection-based method [22].

2.4. Boundary and initial conditions

By exploiting the specific geometry, the model is further simplified by a symmetry condition along the radially oriented *z*-axis. At the lower end of the raceway, a fixed support is defined. Load is respectively applied via a displacement of the two rolling bodies towards the raceway element in the negative *x*-direction. By avoiding a force or surface load, the convergence properties of the numerical procedure are significantly improved. For a general interpretability of the simulation results, the initial state is assumed to be free of (manufacturing) residual stresses.

2.5. Solution

Table 2 presents the four steps, into which two-stage deep rolling is divided in the calculation [23]. This way, the process is correctly simulated to evaluate the induced residual stresses.

Table 2: Solution steps.

Step	Solver task
1	Loading of the raceway with rolling element 1
2	Relieved intermediate situation
3	Loading of the raceway with rolling element 2
4	Relieved final situation

All steps must be executed individually by the solver to achieve the intended result. The previous output respectively serves as starting point of the next calculation part because the solutions are superimposed. Main advantage of this subdivision is that the overall and each individual step result can be viewed in one simulation.

The procedure is implemented by displacement of the first rolling body with respect to the raceway in positive and subsequently negative *x*-direction for load application and relief, respectively. To ensure that the workpiece is not influenced by both tools simultaneously, the other rolling element meanwhile remains at rest by "floating" over its surface. This approach can be transferred to the second load case accordingly. Figure 4 reveals the result of such a simulation. The blue area marks induced compressive residual stresses. The maximum (darkest zone) occurs below the surface, in agreement with the depth distribution of Hertzian contact von Mises equivalent stress.

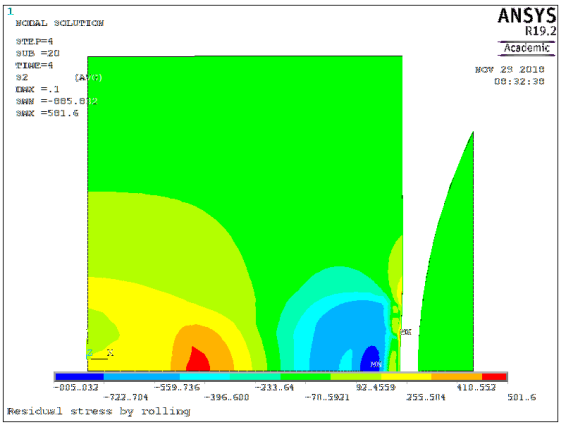

Figure 4: Result of a finite element simulation after step 4, indicating compressive and tensile residual stresses in blue and red, respectively. The rolling (pressing) body is shown on the right, the raceway element on the left. The z-axis is horizontally oriented in the centre of the contact.

3. Results

Before presenting the findings, Table 3-1 provides an overview of the input condition for the performed parameter studies. The two rolling elements of the FEA model are permanently numbered 1 and 2 (see Table 2). This convention emphasizes that each simulation sequence not only involves the corresponding diameters (d_1, d_2) and Hertzian pressures (p_1, p_2) but also the temporal order of loading indicated by an arrow. Table

3-1 thus illustrates the variety of possibilities for applying and (fine-) tuning two-step deep rolling, which makes the present numerical analysis useful for process development and design.

Table 3-1: Scheme of the parameter studies.

Study	Diameter	Hertzian pressure	Order
1	$d_1 > d_2$	$p_1 < p_2$	$1 \rightarrow 2$
2	$d_1 = d_2$	$p_1 < p_2$	$1 \rightarrow 2$
3	$d_1 > d_2$	$p_1 < p_2$	$2 \rightarrow 1$
4	$d_1 > d_2$	$p_1 < p_2$	$2 \rightarrow 1$

Note that contact stresses are not read in directly but calculated by the model (see section 2.4.). Sizes of the rolling elements and (non-round) Hertzian pressures used for the parameter studies are given in Table 3-2.

Table 3-2: Rolling element diameters and applied loads (see Table 3-1).

Study	d_1/mm	d_2/mm	p_1/MPa	p_2/MPa
1	9	5	4716	5266
2	9	9	4013	4161
3	9	5	4799	5121
4	9	5	5083	5121

3.1. Simulation examples

The following diagrams consistently refer to the unloaded condition, as stated in steps 2 and 4 of Table 2. Figure 5-1 shows the result of parameter study 1. The residual stress in circumferential direction is plotted against distance from surface. For the first and subsequent second load case (1, 1→2), respectively, diameters d_1=9 mm and d_2=5 mm are set for the rolling elements. Simulation details are compiled in Tables 3-1 and 3-2. Both surface conditions are adjusted in a way that the final exceeds the initial Hertzian pressure applied, i.e. $p_1<p_2$ (order: 1→2).

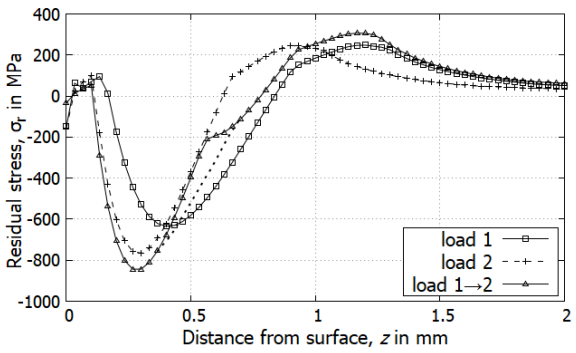

Figure 5-1: Depth profiles of residual stress in circumferential direction, evaluated in the centre of the contact (see Figure 3), for parameter study 1 of Tables 3-1 and 3-2. In addition to the results of initial first (1) and (subsequent) final second (1→2) tool pass, application of load 2 alone (2) is included for reference.

The development of the von Mises residual stress (including plastic material response) in the workpiece raceway for the relieved situations of the analysed two-step deep rolling process of Figure 5-1 (i.e., study 1 of Tables 3-1 and 3-2) is displayed in Figure 5-2. This chart manifests the intended effect on the near-surface zone by the second load (1→2). There is a significant increase of the equivalent stress in the outer layer of $z\leq$0.4 mm, whereas at greater depths changes compared with the previous state are small.

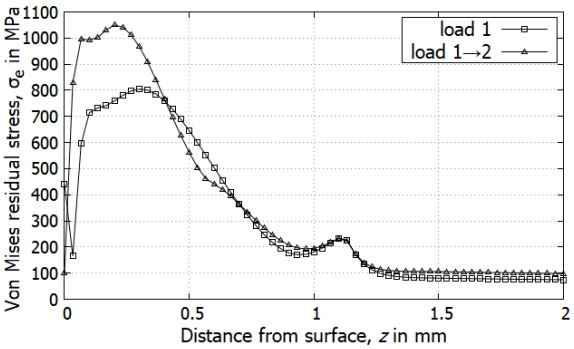

Figure 5-2: Depth distribution of von Mises equivalent residual stress for parameter study 1 (cf. Figure 5-1).

Figure 5-1 indicates that second deep rolling rises the compressive residual stresses substantially near the surface. Due to increased Hertzian pressure ($p_2>p_1$), moreover, the final maximum is about 40% higher.

Mechanical compensation after second loading occurs gradually in the adjacent region. The associated reduction of compressive residual stresses generated previously by the pass of the first rolling element in the inner zone ($z\geq$0.4 mm), however, may be overestimated in the simulation. This assessment is supported by the dashed graph for sole application of load (case) 2, added to Figure 5-1 for comparison. The single-step profiles (1, 2) themselves verify the experimentally well-known correlations that increasing rolling tool diameter expands the impact zone and the position of compression-tension crossover deeper into the material and that larger Hertzian pressures result in higher compressive residual stresses. The nonphysical hump of the terminal curve (1→2) at $z\approx$0.6 mm is related to numerical modelling. The dotted smoothing line assists with estimating the potential benefit of two-step deep rolling according to parameter study 1 over both single-pass processes of load 1 and 2. As the present research focuses on basic correlations, the cause of such obvious numerical inconsistencies (e.g. discretisation) is not further considered. More expanded residual stress redistribution in the second load (pass) mitigates the decrease of the original strengthening depth. This subject is briefly discussed later in the text.

Parameter study 2 of Tables 3-1 and 3-2 aims at indirectly demonstrating the influence of the size of the rolling elements on the residual stresses by choosing both diameters, d_1 and d_2, to be 9 mm. According to the simulation result of Figure 6, the initially induced compressive residual stresses (load 1) are increased and the maximum as well as the inner end of the influence zone are shifted towards larger depth by the second overrolling (1→2) at higher Hertzian pressure. In contrast to Figure 5-1 (study 1), the effect near the surface from the first pass is negligible. Note that the von Mises contact stress for a given Hertzian assembly at any distance (z) increases with load (p_0). In Figure 6, the two-step process (1→2) also does not significantly

raise the impact depth with respect to the included second single-pass reference case (2) of higher pressure. Without shakedown by repeated overturns [1,10], it is the diameter of the rolling element alone that governs the nearest position of subsurface compressive residual stress build-up to a certain magnitude. Expansion of the profile width into the depth for a conventional single tool process occurs only by applying higher Hertzian pressure. Unavoidably associated increase of the compressive residual stress maximum, however, restricts the practical use of this approach. A comparison of both individual load cases (1, 2) in Figure 6 visualizes the basic feature discussed above ($d_1=d_2$, $p_1<p_2$).

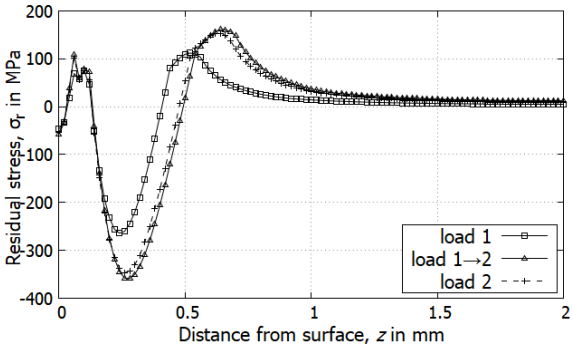

Figure 6: Depth profiles of residual stress in circumferential direction, evaluated in the centre of the contact, for parameter study 2 of Tables 3-1 and 3-2. The distance curve for sole application of load 2 complements the distributions after first (1) and second (1→2) tool pass.

Another accessible influencing factor is the order, in which differently sized rolling elements are applied to the raceway. According to Tables 3-1 and 3-2, parameter studies 1 and 3 are almost identical. It is only the order, in which the larger (1) and smaller (2) rolling element are pressed against the raceway, that actually differs. Figure 7 shows the induced residual stresses after initial (2) and final (2→1) loading. The latter graph is supplemented by a dotted smoothing line (cf. Figure 5-1). The influence depth is significantly increased by the second pass without undesirable changes of the compressive residual stresses in the outer zone.

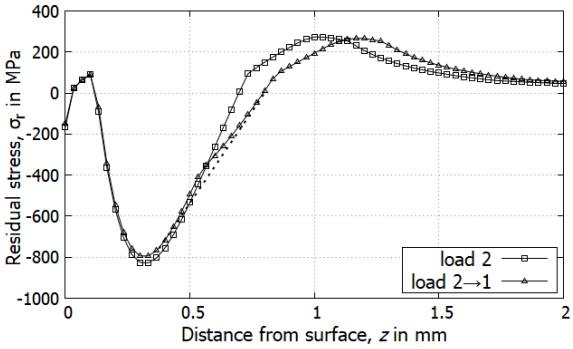

Figure 7: Depth profile of residual stress in circumferential direction, evaluated in the centre of the contact, for parameter study 3 of Tables 3-1 and 3-2.

It is interesting to directly compare the simulation results of study 1 and 3. In Figure 8, the residual stress profiles are smoothed and adjusted at the exit ramp to compensate for numerical inaccuracies. Both curves are rather similar. Whereas Figures 5-1 and 7 illustrate the advantage of two-step deep rolling with regard to improved near-surface coverage and width of the compressive residual stress distributions over the single-stage load 1 and 2 processes, respectively, the suggested increase in efficiency by first applying the large (1→2) rather than the small (2→1) tool needs further investigation for confirmation. Note that the Hertzian pressures of study 1 and 3 are not exactly the same.

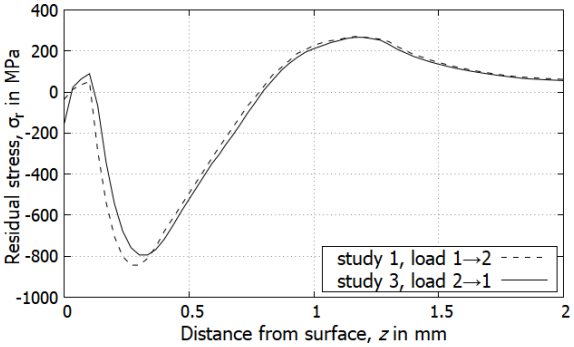

Figure 8: Residual stress comparison of parameter studies 1 and 3 (see Figures 5-1 and 7).

Process performance can finally be tailored effectively by the forces transferred to the raceway through the deep rolling elements. Parameter study 4, defined in Tables 3-1 and 3-2, provides an instructive demonstration. Figure 9 reveals the result of residual stress finite element simulation. The impact of considerably higher final loading than in study 3 (only difference) is obvious from the increased influence depth. As both Hertzian pressures are almost identical ($p_1\approx p_2\approx 5100$ MPa), maximum von Mises contact stresses are either. Hence, the compressive residual stress peaks after load cases 2 and 2→1 are in good agreement (about 800 MPa, note that $p_1<p_2$).

Figure 9 further confirms the benefit of double- over one-step deep rolling. If one refers to the width of the depth zone of compressive residual stress above 400 MPa, this efficiency index rises by a good 50% from 0.38 mm (load 2) to 0.58 mm (2→1). Mutual adjustment of the diameters of the rolling elements and the applied forces (contact pressures), therefore, enables flexible process fine-tuning.

In this context, a last comparison between Figures 6 and 9 is worth drawing. According to Table 3-2, the corresponding parameter studies 2 and 4 reasonably permit distinguishing the effect of an individual tool applied once at two loads onto the raceway surface from a small and large rolling element both employed under the same Hertzian pressure, i.e. $d_1=d_2$, $p_1\neq p_2$ vs. $d_1\neq d_2$, $p_1=p_2$, respectively, on the compressive residual stress distribution. The latter result displayed in Figure 9, therefore, again proves the utility of the upgraded two-step process. Width expansion is completely decoupled from top value enhancement of the residual stress pattern. This influence separation is highly desirable. Note that excessive compressive residual stresses reduce rolling contact fatigue life. For hardened bearing steel, a threshold of about 1000 MPa is reported [24].

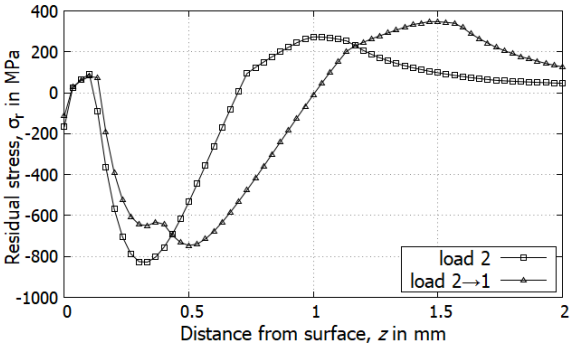

Figure 9: Depth profile of residual stress in circumferential direction, evaluated in the centre of the contact, for parameter study 4 of Tables 3-1 and 3-2.

3.2. Restrictions of the finite element model

A residual stress (σ_r) free initial material condition is assumed in the simulations. In the distance (z) distributions after deep rolling presented above, therefore, compensational redistribution occurs with respect to the $\sigma_r(z)=0$ line. As the workpiece thickness is limited to 3.3 mm in the model, pronounced tension peaks of up to more than 300 MPa are formed after zero crossing. This "overshooting" is just as unrealistic for usual bearing components as exaggerated decrease of compressive residual stresses from first loading in the second pass of two-step deep rolling (see Figure 5-1). Extending the overall thickness of the raceway element, i.e. the distance from surface to fixed support (boundary condition), should further improve the predictions of the finite element analysis.

4. Conclusions

Improvement of product performance is an important driver of technology innovation. Deep rolling for inducing compressive residual stresses in the Hertzian fatigue and friction loaded edge zone currently experiences growing interest in bearing applications. The method of moving a round pressing tool (ball or roller) over the surface of a workpiece is similar to low plasticity burnishing. Advanced computer simulations play a progressive role in process development. In this paper, a finite element analysis using ANSYS is carried out to simulate a two-step deep rolling operation. The intention is to estimate the potential for optimizing the compressive residual stress distribution by smartly combining differently sized and loaded tools. A simplified two-dimensional contact model with bilinear elastic-plastic isotropic material behaviour of the treated bearing steel is created and discussed. The studied parameter constellations include diameters and order of application of the rolling elements as well as Hertzian pressure on the workpiece raceway surface. The effect on width and intensity of the resulting residual stress field is investigated.

High operating speed, cleanliness and combinational variety (e.g. with turning) as well as involved surface smoothing make deep rolling an attractive mechanical strengthening process. Edge weakness of the induced compressive residual stress distribution, however, is a well-known challenge in conventional single-tool practice. Corrective measures proposed in the literature to mitigate this process-inherent disadvantage are discussed. A schematic single-pass deep rolling residual stress profile is depicted in Figure 10. The graph is used to quantify the undesirable skin. With respect to a lower (effectiveness) reference level σ_0 of compressive residual stress, for instance 400 MPa, the weaker boundary layer extends from the surface to a depth z_1. The width of the actual strengthening zone, Δz, thus amounts to $z_2–z_1$. It is worth noting for a single-pass process that the depths $z_1(d)$ and $z_2(p_0)$, respectively, depend essentially on the rolling element diameter d and the applied Hertzian pressure p_0, which is restricted by the material-specific threshold σ_{th} (about 1000 MPa for bearing steel) of maximum (beneficial) compressive residual stress $\sigma_{r,max}(p_0)\leq\sigma_{th}$. Figure 10 concisely illustrates the intrinsic restriction of single-tool/pass deep rolling. It, however, also suggests the approach adopted in the present paper. The numerical simulations indicate that effective width expansion and shape equalization of the compressive residual stress profile can be achieved by the use of two differently sized rolling elements and the application of similar Hertzian pressures, respectively. Note that larger variation in both tool diameters ($\Delta d=|d_1–d_2|$) further increases the influence range Δz. The load on the smaller, near-surface impacting rolling element affects residual stress redistribution in the depth.

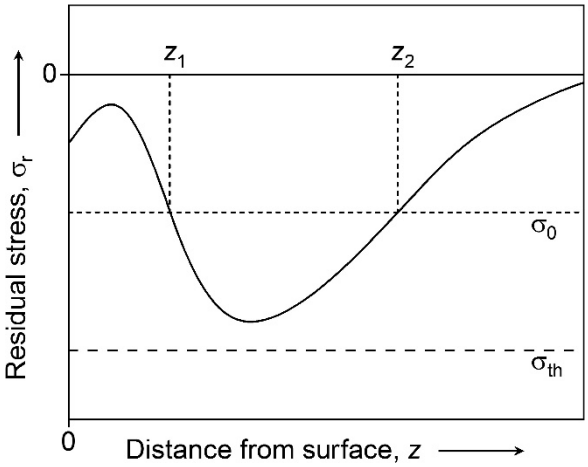

Figure 10: Schematic representation of the residual stress depth profile from single-pass (one tool) deep rolling.

Track widths of differing balls may strongly deviate from each other. A combination (tool) of a small and a large cylindrical roller is therefore easier to use with the proposed two-step process. When applying balls on curved surfaces, however, optimization of the compressive residual stresses only in the (often) highest loaded radius region can be sufficient.

The four finite element parameter studies presented in this paper allow fundamental statements about multi-stage deep rolling. Tool sizes and Hertzian pressures prove to be versatilely appropriate process variables for residual stress engineering. The influence of application order of different rolling elements is not yet

fully clarified but simulations hint at benefit from primarily large and subsequently small diameter. So prepared experimental series are intended for providing further insight into optimized design and fine-tuning of two-pass deep rolling compressive residual stress profiles. The magnitude of an involved increase in hardness H by cold working depends on the heat treatment and mechanical material history. It is of minor relevance to bearing steel condition of $H \geq 58$ HRC. The effect, however, is amplified with decreasing original hardness. Unlike compressive residual stress, no local (redistribution) loss accompanies the second overturn.

Acknowledgment

The authors are grateful to Dr. Werner Horn, SKF Advanced Engineering Competence Centre, for his support and helpful discussions. Permission to publish by SKF is appreciated.

References

[1] S. S. Cretu, M. I. Benchea, O. S. Cretu: Compressive Residual Stresses Effect on Fatigue Life of Rolling Bearings. Proc. IMECE07, 2007 ASME International Mechanical Engineering Congress and Exposition, 11–15 November 2007, Seattle, Washington, USA, American Society of Mechanical Engineers, New York, 2008, pp. 485–490.

[2] A. Pabst, S. Tremmel, S. Wartzack: Investigation of residual compressive stresses in rolling bearing components and their impact on the rating life. Proc. 69th STLE Annual Meeting and Exhibition, 18–22 May 2014, Lake Buena Vista, Florida, USA, Society of Tribologists and Lubrication Engineers, Park Ridge, Illinois, USA, 2014, Vol. 1, pp. 475–478.

[3] F. Pape, O. Maiß, B. Denkena, G. Poll: Computational approach to improve bearings by residual stresses based on their required bearing fatigue life. Int. J. Comp. Meth. and Exp. Meas., Vol. 6, 2018, No. 4, pp. 656–666.

[4] T. Coors, F. Pape, G. Poll: Comparing the Influence of Residual Stresses in Bearing Fatigue Life at Line and Point Contact. Materials Research Proceedings, Vol. 6, 2018, pp. 215–220.

[5] W. Grzesik, K. Zak, M. Prazmowski: Surface Integrity of Hard Turned Parts Modified by Ball Burnishing. J. Mach. Eng., Vol. 12, 2012, No. 1, pp. 18–27.

[6] M. Brückner, J. Gegner, A. Grabulov, W. Nierlich, J. Slycke: Butterfly Formation Mechanisms in Rolling Contact Fatigue. Proc. VHCF-5 (edited by C. Berger, J. Christ), 5th International Conference on Very High Cycle Fatigue, 28–30 June 2011, Berlin, Germany, DVM Deutscher Verband für Materialforschung und -prüfung, Berlin, Germany, pp. 101–106.

[7] J. Gegner, W. Nierlich: Service Loading of Rolling Bearings in Wind Turbine Gearboxes: X-ray Diffraction Material Response Analysis of White Etching Cracks Premature Failures. Tribol. Trans., Vol. 61, 2018, No. 2, pp. 269–278.

[8] J. Fella, O. Beer: Verfahren zur Herstellung von Wälzlagerringen und Wälzlager. German Patent, DE 102015207779A1, filed 28 Apr. 2015.

[9] P. S. Prevey, J. E. Haas: Method and apparatus for improving the distribution of compressive residual stress. United States patent application, US 2008/0081208A1, filed 24 Sept. 2007.

[10] J. Gegner: Verfahren zum Festwalzen eines metallischen Objekts, insbesondere einer Laufbahn eines Wälzlagers. German patent, DE 102015201644B4, filed 30 Jan. 2015.

[11] X. Cheng: Experimental and numerical approaches for improving rolling contact fatigue of bearing steel through enhanced compressive residual stress. PhD thesis, Ohio State University, Columbus, Ohio, 2007.

[12] N. Lyubenova, D. Bähre: Investigation of the surface residual stresses in single and multiple trace deep rolling on flat AISI 4140 specimens. Proc. ICSP-13, 13th International Conference on Shot Peening, 18–21 Sept. 2017, Montreal, Quebec, Canada, pp. 428–433.

[13] N. Lyubenova, D. Bähre: Finite Element Modelling and Investigation of the Process Parameters in Deep Rolling of AISI 4140 Steel. J. Mater. Sci. Eng. B, Vol. 5, 2015, No. 7–8, pp. 277–287.

[14] J. Gegner, U. Krug, A. Olschwski, A. Stubenrauch: Method for producing a track element of a bearing assembly. United States patent, US 9273727B2, filed 25 Oct. 2012.

[15] W. Rust: Nichtlineare Finite-Elemente-Berechnungen: Kontakt, Geometrie, Material. 2nd edition, Vieweg+Teubner, Wiesbaden, Germany, 2011, pp. 235–264.

[16] S. M. Hassani-Gangaraj, M. Carboni, M. Guagliano: Finite element approach toward an advanced understanding of deep rolling induced residual stresses, and an application to railway axles. Mater. Des., Vol. 83, 2015, pp. 689–703.

[17] N. Lyubenova, M. Jacquemin, D. Bähre: Influence of the Pre-Stressing on the Residual Stresses Induced by Deep Rolling. Materials Research Proceedings, Vol. 2, 2016, pp. 253–258.

[18] L. G. A. Fonseca, A. R. de Faria: A deep rolling finite element analysis procedure for automotive crankshafts. J. Strain Anal. Eng., Vol. 53, 2018, No. 3, pp. 178–188.

[19] E. Broszeit, T. Preussler, M. Wagner, O. Zwirlein: Stress Hypotheses and Material Stresses in Hertzian Contacts. Z. Werkstofftech., Vol. 17, 1986, No. 7, pp. 238–246.

[20] J. Gegner, W. Nierlich: Comparison of the Microstructural Changes and X-ray Diffraction Peak Width Decrease during Rolling Contact Fatigue in Martensitic Microstructures. Bearing Steel Technologies, Vol. 9, Advances in Rolling Contact Fatigue Strength Testing and Related Substitute Technologies (edited by J. M. Beswick), Selected Technical Papers, STP 1548, ASTM International, West Conshohocken, Pennsylvania, USA, 2012, pp. 303–328.

[21] L. Nasdala: FEM-Formelsammlung Statik und Dynamik: Hintergrundinformationen, Tipps und Tricks. 3rd edition, Springer, Wiesbaden, Germany, 2015, pp. 227–235.

[22] ANSYS Inc.: ANSYS Mechanical APDL Contact Technology Guide. Canonsburg, Pennsylvania, USA, 2016, pp. 15–60.

[23] J. Simon: Finite-Elemente-Analyse des Druckeigenspannungsaufbaus beim stufenweisen Festwalzen. Bachelorthesis, University of Applied Science Würzburg-Schweinfurt, Schweinfurt, Germany, 2019, pp. 46–50.

[24] E. Schreiber, W. Simon, H.-W. Zoch: Work Hardening of Ball Surfaces. Creative Use of Bearing Steels (edited by J. J. C. Hoo), Selected Technical Papers, STP 1195, ASTM International, West Conshohocken, Pennsylvania, USA, 1993, pp. 81–92.